Enhanced Patterned Wafer Defect Detection for the 7 nm Node Using a 405nm Laser based Metalens Array

Jinlong Zhu *, **Sanyogita Purandare**, and **Lynford L. Goddard** *

*Email: lgoddard@illinois.edu; zhuwdwz1@illinois.edu   PSL Group: http://psl.mntl.Illinois.edu/
Photonic Systems Laboratory, Department of Electrical and Computer Engineering, University of Illinois at Urbana-Champaign, Urbana, USA

INTRODUCTION

With the current critical dimension (CD) in patterned wafers approaching sub-10 nm in the next few years, it has become quite challenging to accurately detect killer defects without sacrificing the inspection speed needed by the high-volume manufacturing semiconductor industry. Consider that optical methods are nondestructive and can inspect a large pattern area in a single shot, they automatically fulfill most of the rigid industrial requirements. **However, the signal strength from Rayleigh scattering scales as D^6/λ^4 where D is the defect size and λ is the illumination wavelength. Consequently, when the transverse dimensions are smaller than 10 nm, light can only stimulate an extremely weak signal that will be easily submerged by numerous noise sources such as imperfections in the optical system or on-wafer roughness** [1, 2]. This bottleneck, to date, remains unsolvable in the scope of far-field optical inspection. Hence, it is vital to develop an optical system that can balance enhance the signal strength in order to meet most of the rigid requirements in semiconductor inspection.

In this article, we introduce the near-field metalens array into a conventional bright-field optical system to meet the grand challenge of patterned wafer inspection.

CHALLENGES

Backgrounds and Challenges:

a) Shrinkage in the lateral pitch and critical dimensions of patterned features
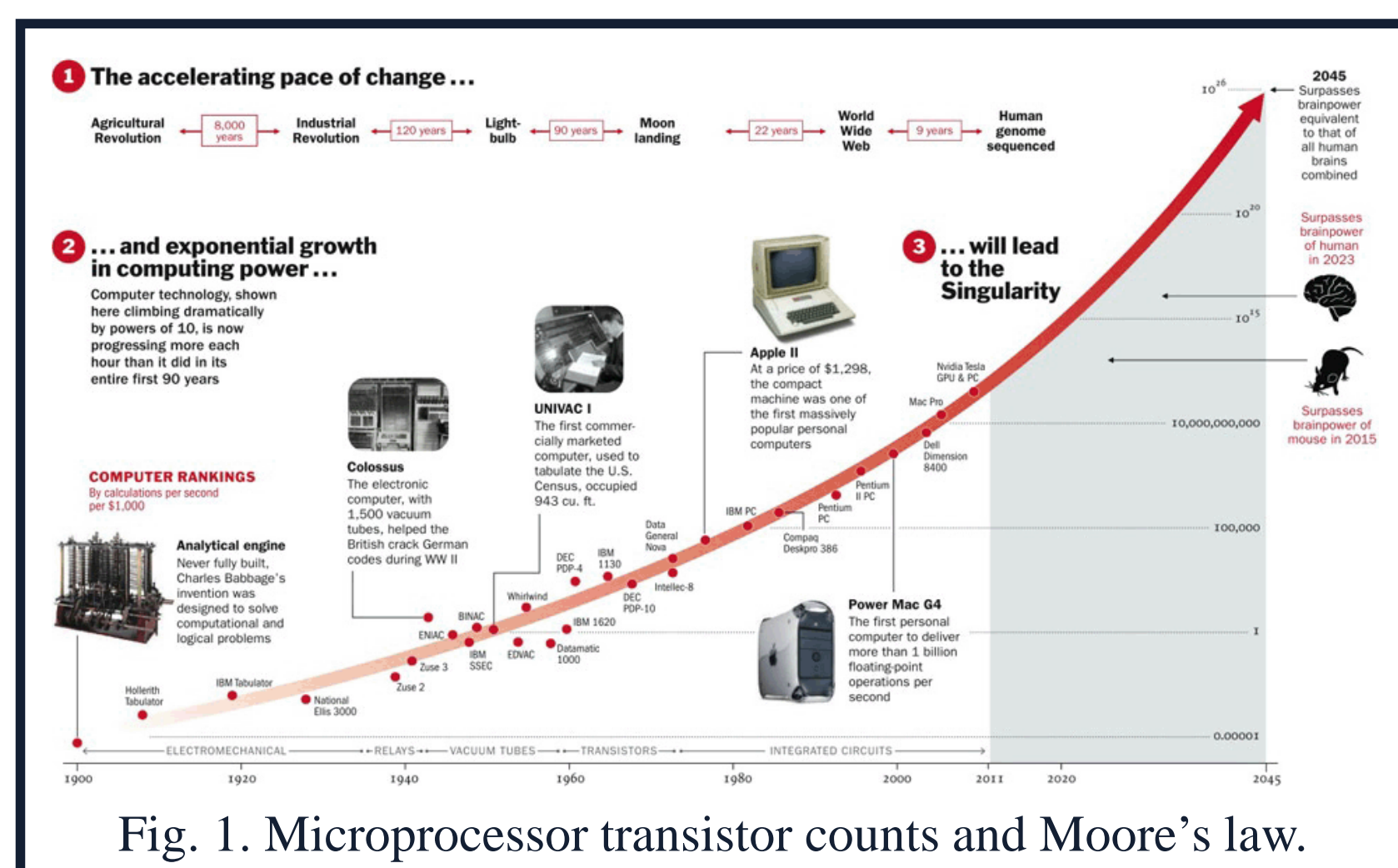

Fig. 1. Microprocessor transistor counts and Moore's law.

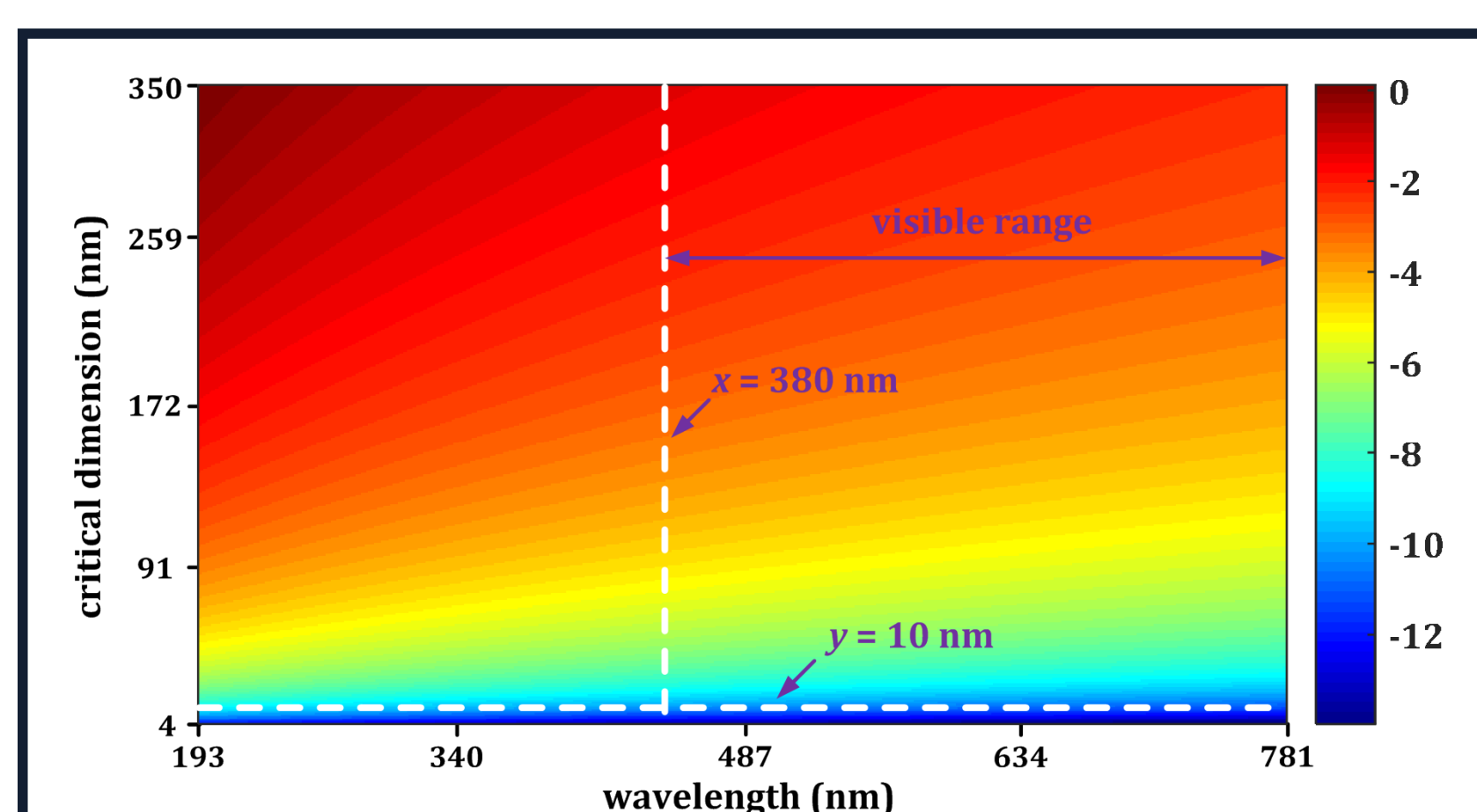b) Extremely weak signal of killer defects (sub-10 nm) stimulated by lasers with wavelength above 193 nm

Fig. 2. Sensitivity map (in log scale) associated with the equation of Rayleigh scattering cross-section.

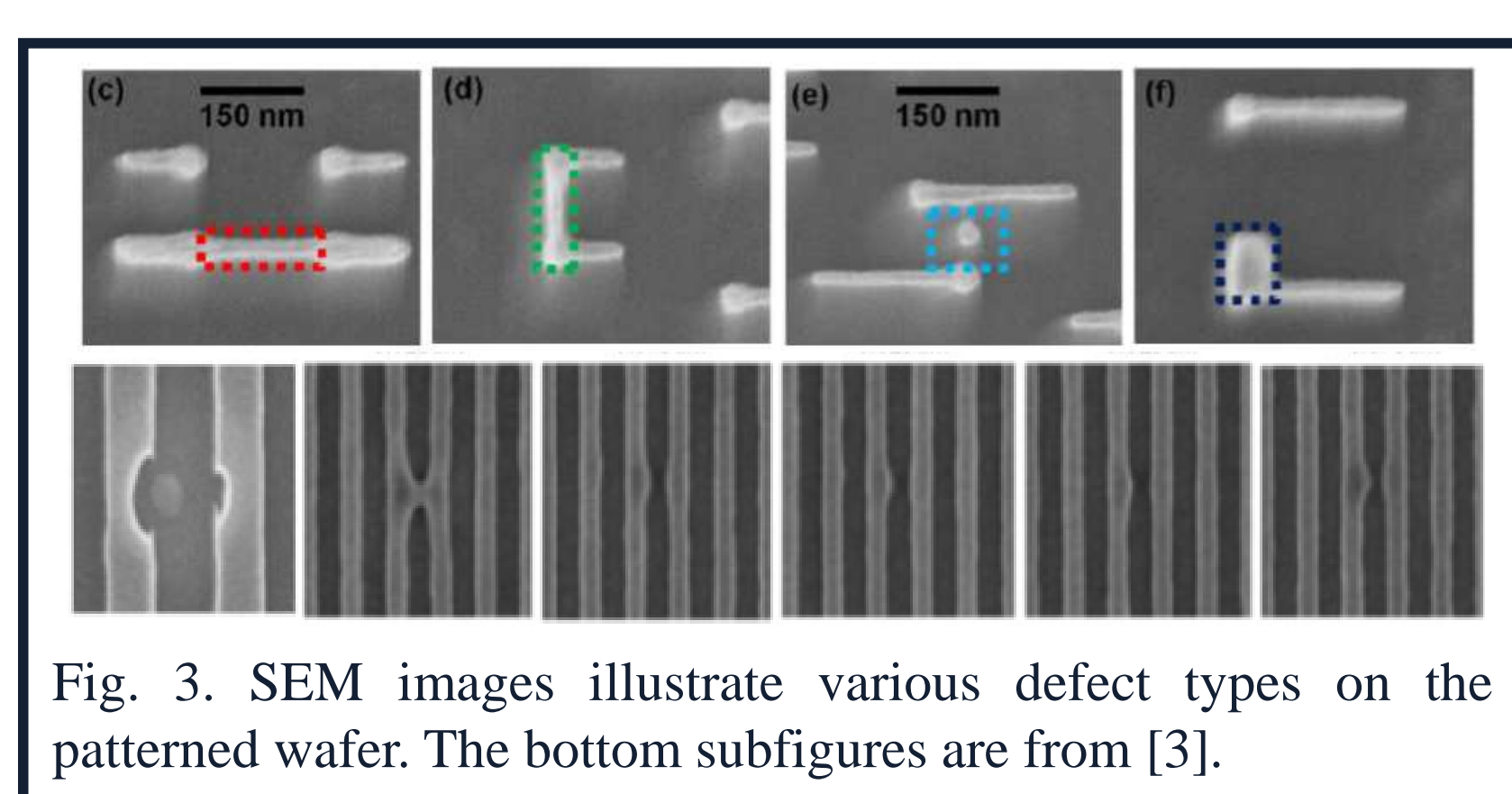c) Detection and classification of killer defects

Fig. 3. SEM images illustrate various defect types on the patterned wafer. The bottom subfigures are from [3].

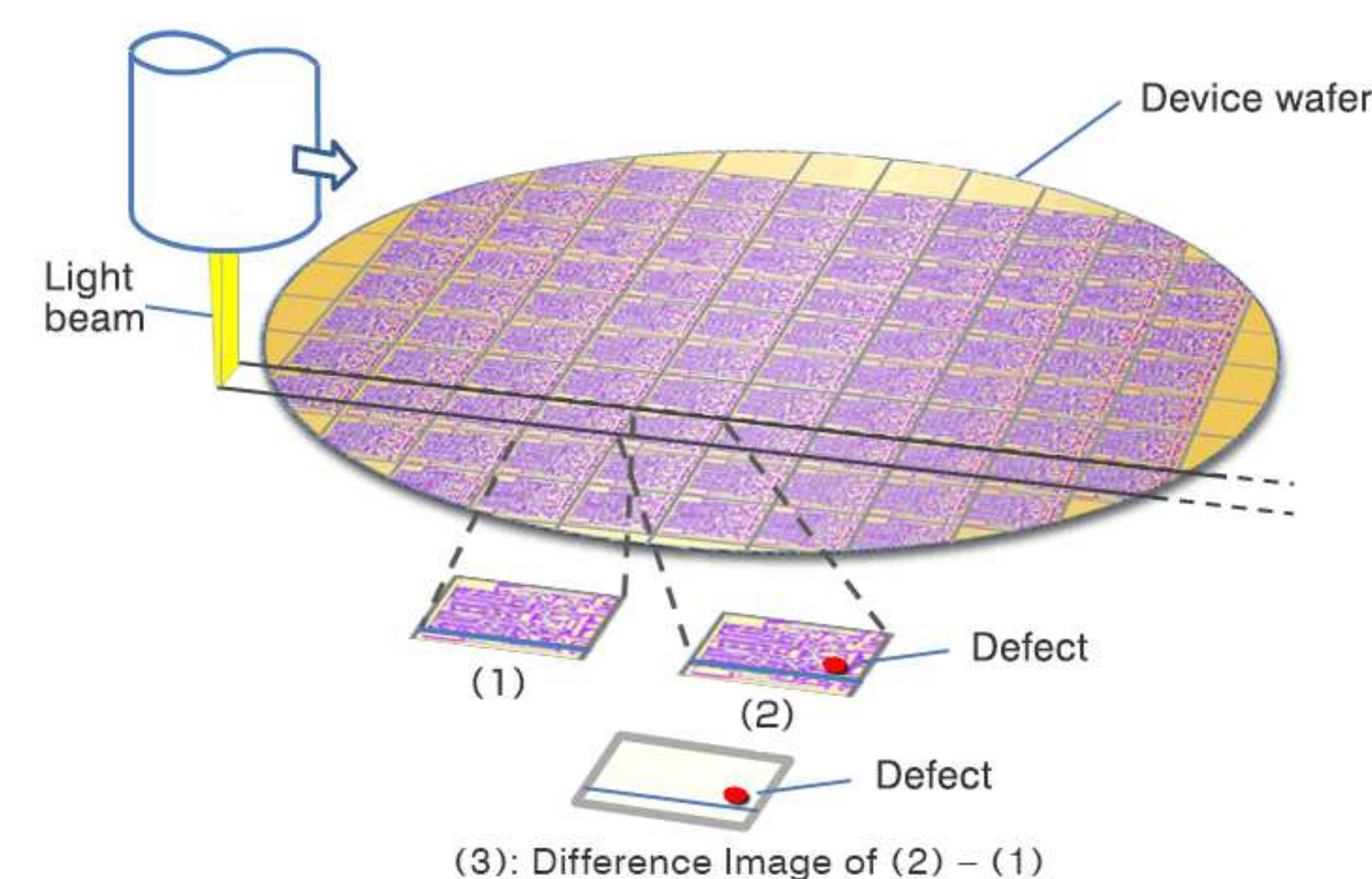## BRIGHT-FIELD INSPECTION MODELING

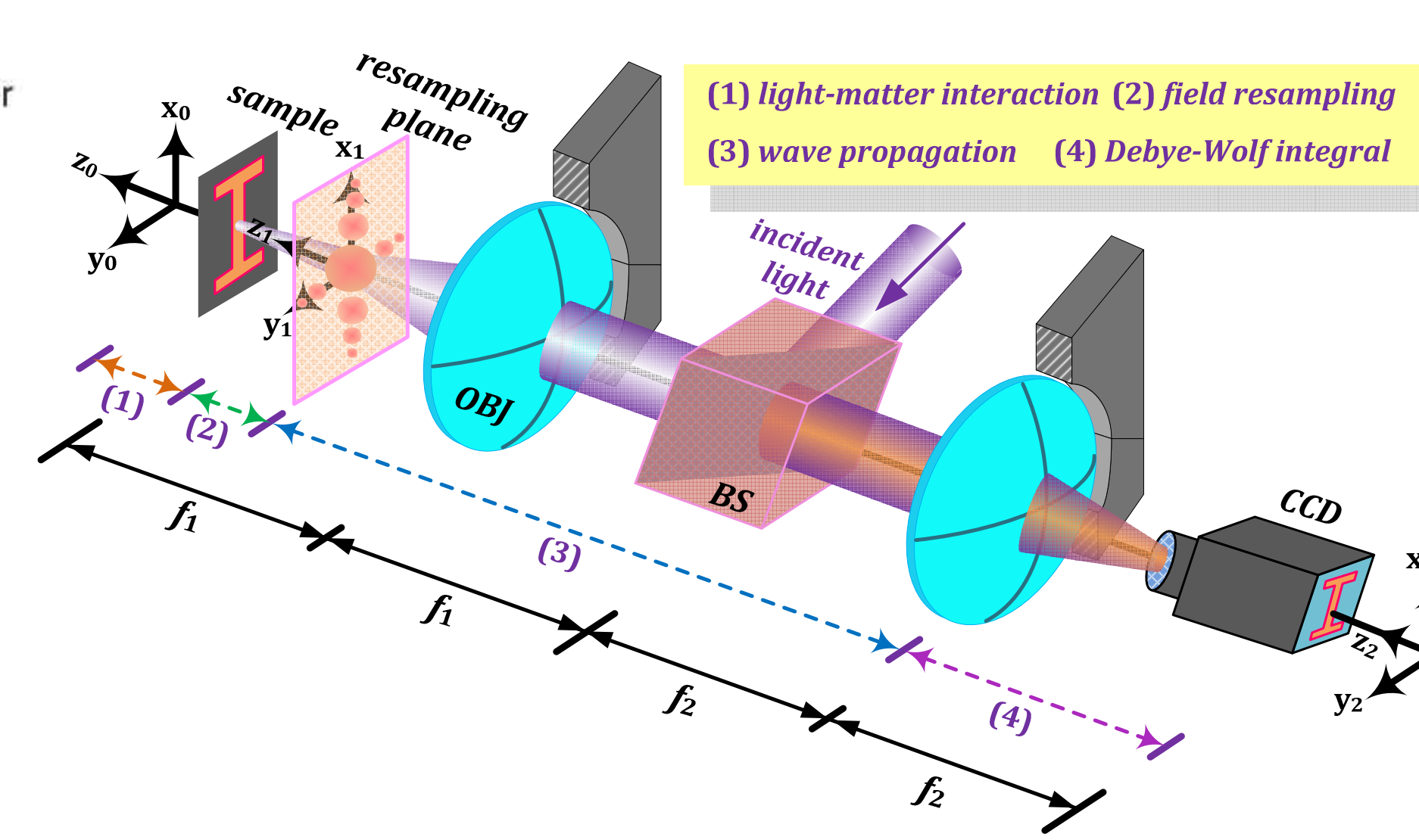Fig. 4. Principles of defect detection on a patterned wafer. Figure is from [4].

Fig. 5. Diagrammatic description of the systematic simulation model for computing the image of an arbitrary object in an epi-illumination coherent optical microscope. The wavelength is fixed at 405 nm throughout the paper.

The First Patterned Wafer :

a) 40 × 9 unit cells; critical dimension = 28 nm; Λ_x = 240 nm, Λ_y = 330 nm
b) incident angle θ = 0 deg. ; azimuthal angle φ = 0 deg. ; polarization angle γ = 0 or 90 deg.
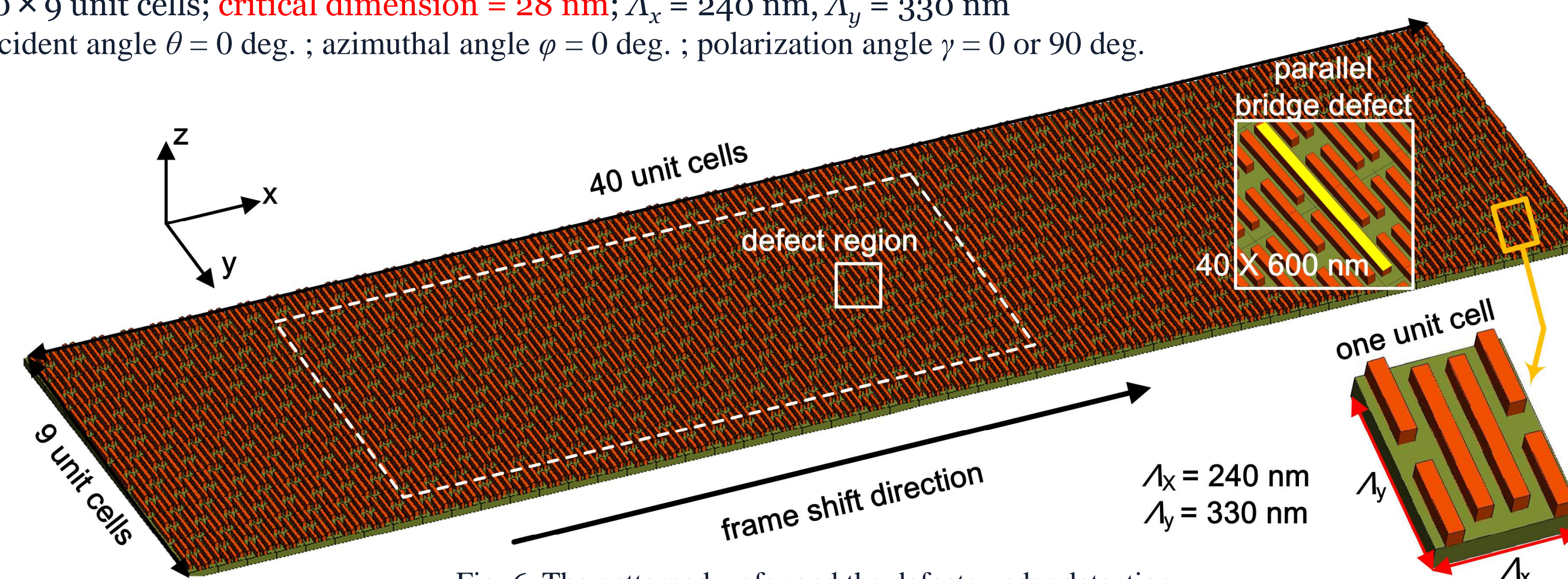

Fig. 6. The patterned wafer and the defects under detection.

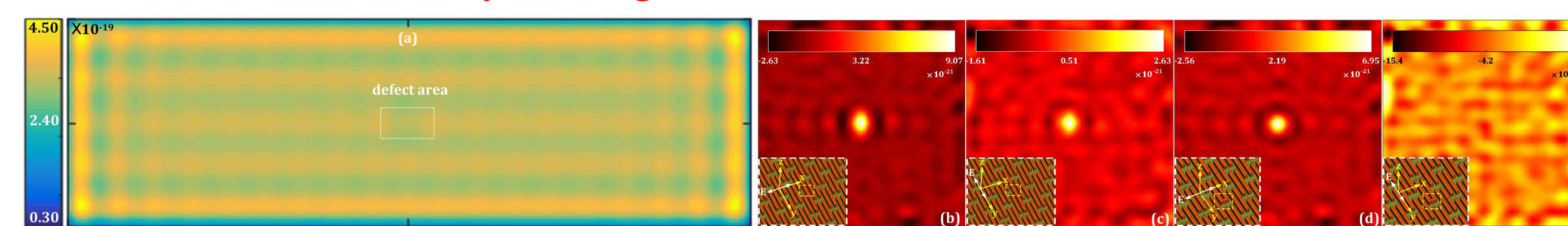**Extremely weak signal even for a defect with a 28 nm CD!**

Fig. 7. (a) Amplitude image with respect to the entire wafer containing a parallel bridge defect under perpendicular polarization illumination. Differential intensity maps associated with the parallel bridge defect under (b) parallel and (c) perpendicular polarization illumination. (d) and (e) corresponding figures for the perpendicular bridge defect.

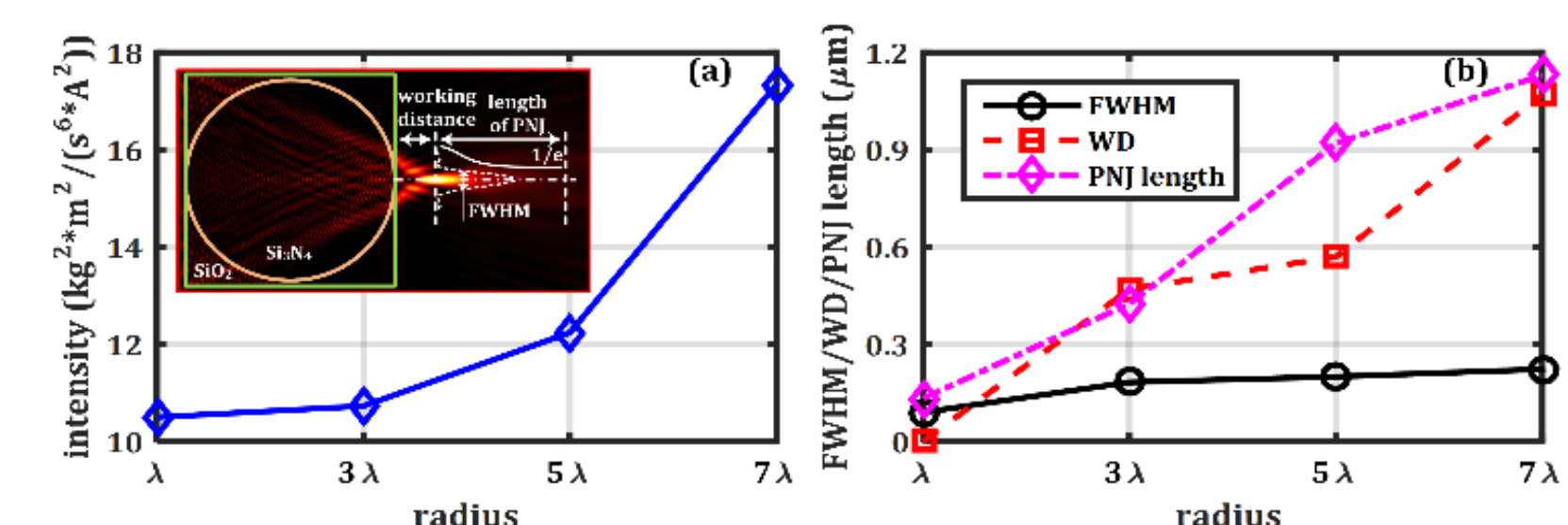## ENHANCED DEFECT INSPECTION

Design of the Metalens:

Fig. 8. The (a) maximal intensity and (b) length parameters (FWHM/WD/PNJ length) of the focused beams corresponding to different radiuses of a microfiber. The bottom axes of all the subfigures have been normalized by the illumination wavelength.
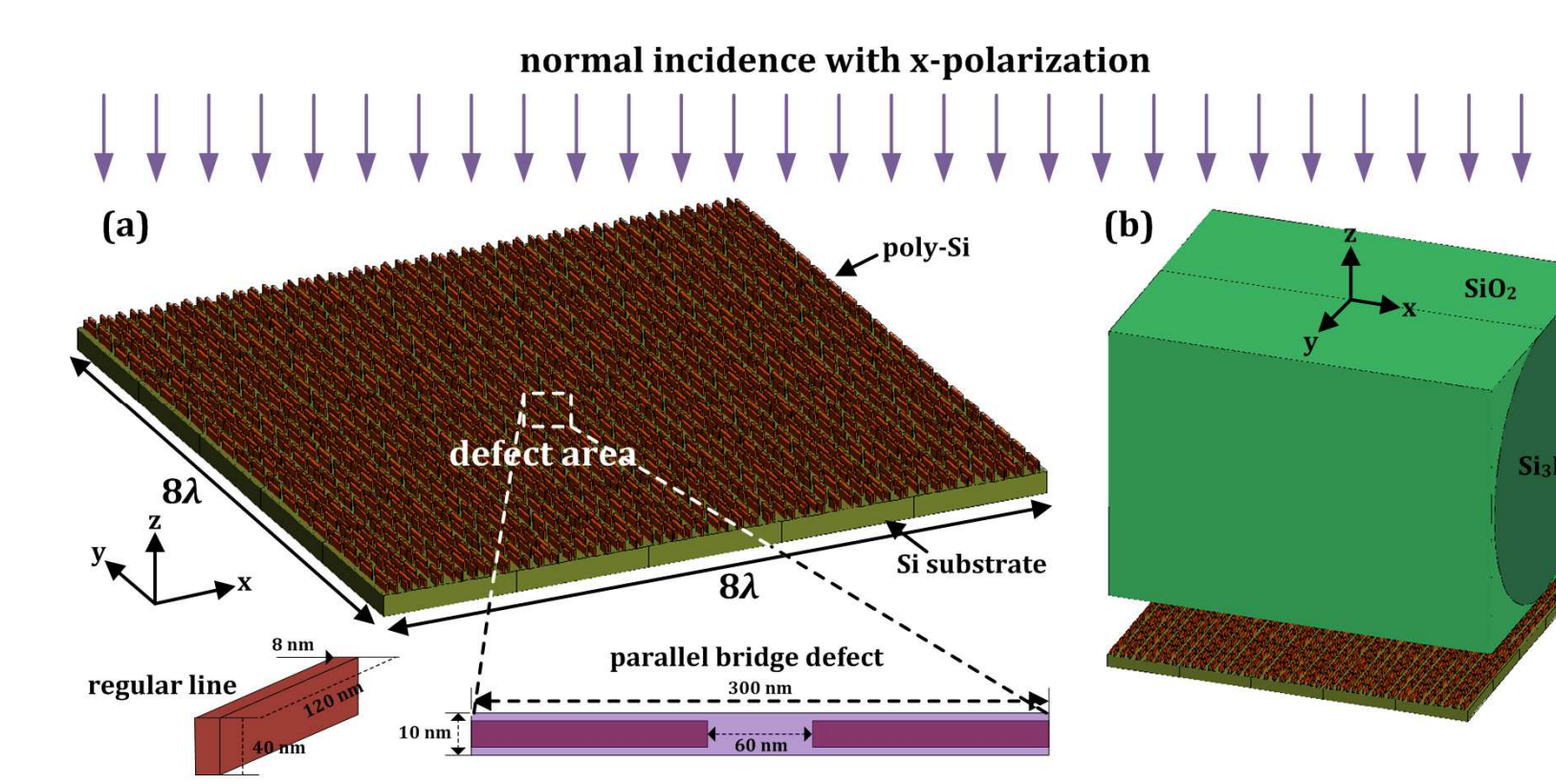

Fig. 9. (a) Geometries of the second patterned wafer and the regular line as well as the parallel bridge defect. (b) Measurement setup of the metalens based defect inspection system. Here the radius of the microfiber is fixed at 3λ.
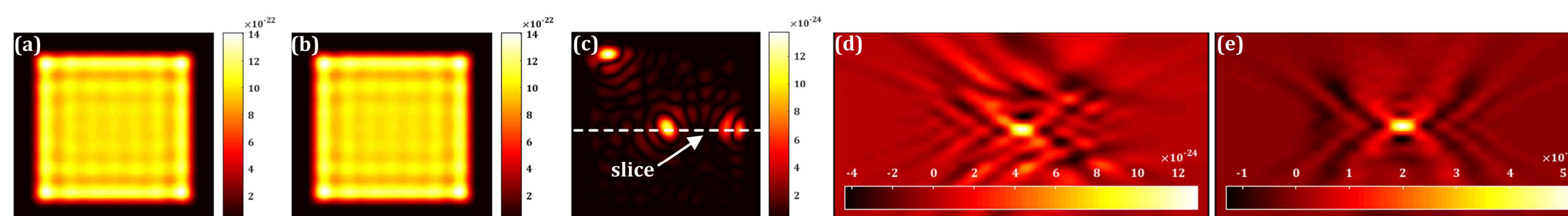

Fig. 10. Simulated in-focus images for the conventional bright-field microscope for the sub-10 nm nanostructure (a) with and (b) without the parallel bridge defect. The polarization of the **E** field of the normally incident plane wave is along x direction. (c) Differential image obtained by subtracting Fig. 10(a) from 10(b). Through-focus differential images (TFDI) corresponding to the (d) x-polarization and (e) y-polarization.

Note:
CCD captures the absolute magnitude of the scattering field

$$\frac{\text{Max}_{TFDI\ y\ polar}}{\text{Max}_{TFDI\ x\ polar}} = \frac{5.30 \times 10^{-23}}{1.30 \times 10^{-23}} = 4.08$$
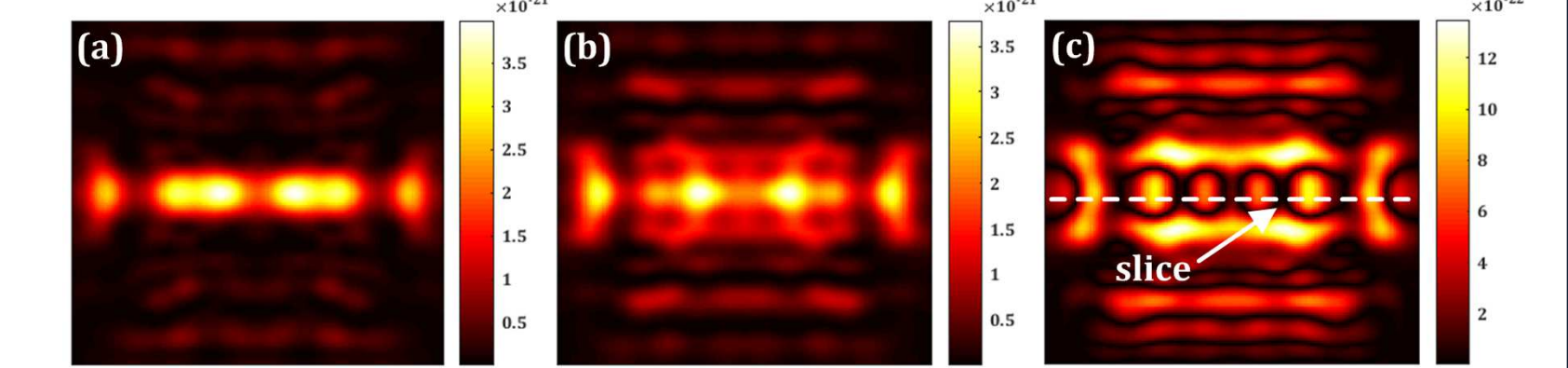
CONTINUED

Fig. 11. The in-focus images for the metalens assisted microscope for the 7nm node patterned wafer corresponding to the cases (a) without and (b) with the parallel bridge defect. (c) Differential image obtained by subtracting Fig. 11(a) from 11(b).
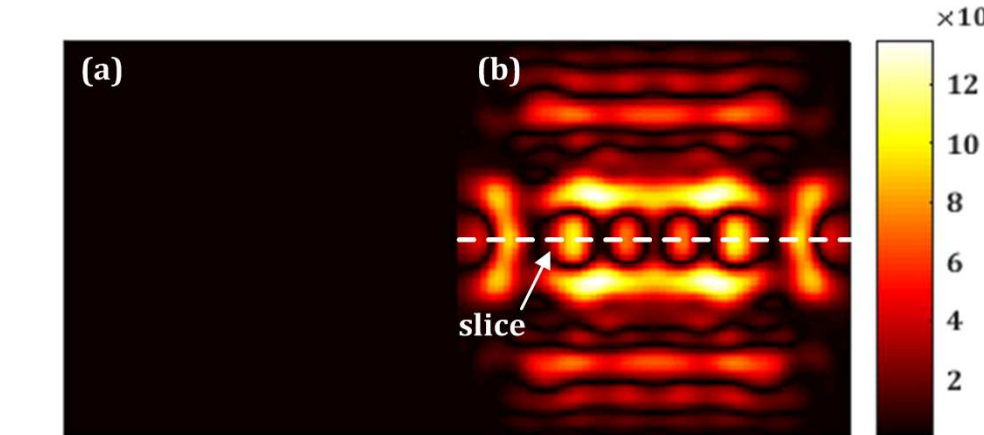

Fig. 12. The far-field signatures associated with the defect under x-polarization normal illumination using (a) a conventional coherent optical microscope and (b) the metalens assisted optical system. Subfigures 12(a) and 12(b) are the same as Figs. 10(c) and 11(c), respectively.
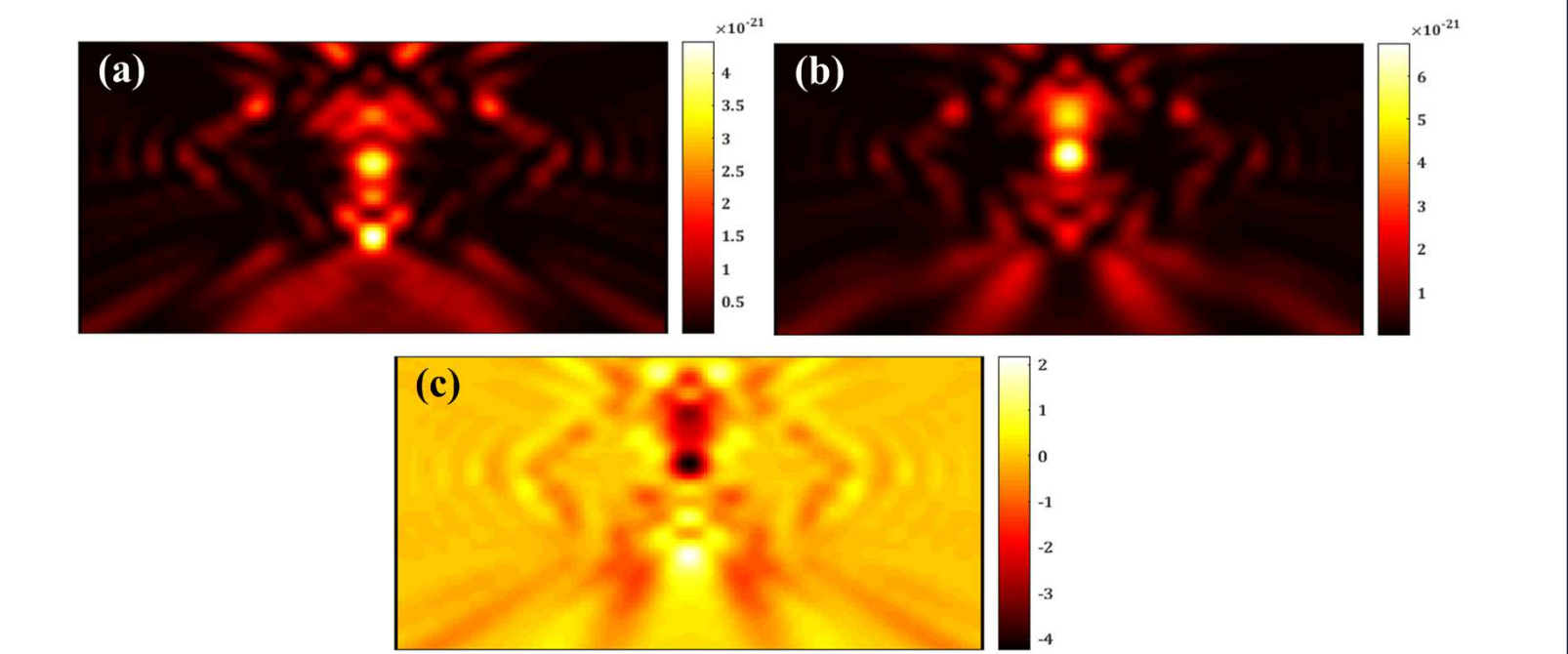

Fig. 13. Through-focus images of the patterned wafer corresponding to the cases (a) without and (b) with the parallel bridge defect for the metalens assisted microscope. (c) TFDI obtained by subtracting Fig. 13(a) from 13(b).

Fig. 14. Comparison for showing the signal enhancement by the proposed inspection system. Subfigures 14(a) and 14(b) are the same as Figs. 10(d) and (e), respectively. Fig. 14(c) is obtained by changing Fig. 13(c) into absolute values.

$$\frac{\text{Max}_{Meta\ TFDI\ x\ polar}}{\text{Max}_{Conv\ TFDI\ x\ polar}} = \frac{4.25 \times 10^{-21}}{1.30 \times 10^{-23}} = 326.9$$

$$\frac{\text{Max}_{Meta\ TFDI\ x\ polar}}{\text{Max}_{Conv\ TFDI\ y\ polar}} = \frac{4.25 \times 10^{-21}}{5.30 \times 10^{-23}} = 80.2$$

The peak defect signature for the proposed system is two orders of magnitude greater than that associated with the conventional setup! Moreover, the metalens is an add-on and thus backwards compatible with conventional systems.

ACKNOWLEDGMENTS

REFERENCES

1. B. M. Barnes, M. Y. Sohn, F. Goasmat, H. Zhou, A. E. Vladar, R. M. Silver, and A. Arceo, *Optics Express* **21**, 26219-26226 (2013)..
2. J. Zhu, K. Zhang, N. Davoudzadeh, X. Wang, and L. L. Goddard, "Electromagnetic field modeling for defect detection in 7 nm node patterned wafers," *Proc. SPIE* **9778**, 97780P (2016).
3. http://www.nanowerk.com/news/newsid=21050.php
4. http://www.hitachi_hightech.com/global/products/device/semiconductor/inspection.html.

ILLINOIS
UNIVERSITY OF ILLINOIS AT URBANA-CHAMPAIGN